Observation of an emissive intermediate in a liquid singlet fission and triplet fusion system at room temperature

Jiale Feng,[†,⊥] Parisa Hosseinabadi,[‡,⊥] Damon M. de Clercq,[†] Michael. P. Nielsen,[‡] Matthew W. Brett,[†] Shyamal K. K.Prasad,[†] Abbas D. Farahani,[¶] Hsiu L. Li,[¶] Samuel N. Sanders,[§] Jonathon E. Beves,[†] N. J. Ekins-Daukes,[‡] Jared H. Cole,[‖] Pall Thordarson,[¶] Murad J. Y. Tayebjee,[‡] and Timothy W. Schmidt[*,†]

†*ARC Centre of Excellence in Exciton Science, School of Chemistry, UNSW Sydney, NSW 2052, Australia*

‡*School of Photovoltaic and Renewable Energy Engineering, UNSW Sydney, NSW 2052, Australia*

¶*The UNSW RNA Institute, The Australian Centre for Nanomedicine, School of Chemistry, UNSW Sydney, NSW 2052, Australia*

§*Rowland Institute at Harvard University, Cambridge, MA 02142, USA*

‖*ARC Centre of Excellence in Exciton Science, School of Science, RMIT University, Melbourne, VIC 3001, Australia*

⊥*Contributed equally to this work*

E-mail: timothy.schmidt@unsw.edu.au

Abstract

The photophysical processes of singlet fission and triplet fusion have numerous emerging applications. They respectively involve the separation of a photo-generated singlet exciton into two dark triplet excitons and the fusion of two dark triplet excitons into an emissive singlet exciton. The role of the excimer state, and the nature of the triplet-pair state in these processes have been a matter of contention. Here we carefully analyse the room temaperature time-resolved emission of a neat liquid singlet fission chromophore, 5,12-bis(*n*-octyldiisopropylsilylethynyl)tetracene. It is demonstrated to exhibit three spectral components:

Two that correspond to the bright singlet and excimer states, and a third component that becomes more prominent during triplet fusion. A spectrum consistent with this third compoment is found to be enhanced with magnetic fields, confirming its origins in radiation from weakly-coupled triplet pairs. This magnetically enhanced emission is attributed to the emission from the strongly coupled triplet pair state. These observations serve to unite the view that there is an emissive intermediate in singlet fission and triplet fusion, and that this species is distinct from the broad, unstructured excimer emission.

Singlet fission (SF)[1] and triplet fusion (TF)[2] are related photophysical processes with promising applications spanning photovoltaics,[3–5] photocatalysis,[6] optical and magnetic resonance imaging,[7,8] multiexcitonic logic[9,10] and advanced manufacturing.[11] In photovoltaics, these processes offer the possibility of much higher limiting efficiencies compared to single-threshold solar cells.[3,12–14] In SF, a photo-prepared excited singlet state couples to a ground state chromophore and transfers about half its energy, ultimately bringing about two uncoupled chromophores in their lowest-energy triplet states.[1] The system conserves spin, and is widely accepted to traverse a region of the potential energy landscape corresponding to a singlet-coupled triplet pair state, $^1(\mathrm{TT})$, with exchange coupling much greater than the zero-field splitting of the individual triplet states.[15–17] As the triplets move apart, the exchange coupling diminishes and the spin identity of the bichromophoric state is lost.[18] These weakly-coupled triplets may return to the singlet manifold by the process of TF.[2,18,19]

In TF, the reverse process occurs whereby weakly-coupled triplets become more strongly coupled before crossing to the highly emissive excited singlet state.[2] In concentrated solutions, aggregates and films, the excited singlet state may form an excimer, corresponding to a deep well on the potential energy surface brought about by strong excitonic coupling. The interplay between the excited singlet, S_1, the excimer, $^1\mathrm{Ex}$, and the $^1(\mathrm{TT})$ state has been the subject of debate.[19–27] In concentrated solutions of 5,12-bis((triisopropylsilyl)ethynyl)tetracene (TIPS-Tc) and 6,13-bis((triisopropylsilyl)ethynyl)pentacene (TIPS-Pc) it has been asserted that the excimer con-

stitutes an intermediate in SF.[20,21] However, Dvořák *et al.* showed using total internal reflection excitation that concentrated TIPS-Pc solutions do not exhibit an emissive excimer.[22] Furthermore, through careful analysis the time-resolved photoluminescence of concentrated TIPS-Tc solutions, Dover *et al.* demonstrated that the excimer, evidenced by a featureless and red-shifted emission spectrum, served as a trap, and that triplets could be generated from the S_1 state without necessarily accessing the excimeric well.[19] Recently, Bossanyi *et al.* countered to show that in pentacene single crystals and anthradithiophene films at 100 K, a red-shifted spectrum, distinct from the excimer, evinced an emissive intermediate state in triplet fusion which they labeled as $^1(\mathrm{TT})$. Such a weakly emissive state was previously observed in low temperature tetracene thin films.[28,29] The $^1(\mathrm{TT})$ intermediate has been the subject of a number of other reports in aggregates and films of acene derivatives.[15,30–35] This begs the question, can such a third, emissive state be observed in SF liquids or solutions? Such an observation would unite models of SF across different phases at device-relevant temperatures. Furthermore, such a spectrum should be enhanced by magnetic fields, which are know to attenuate SF to free triplets.[36,37]

To illuminate this question, we synthesised a room temperature liquid SF material 5,12-bis(n-octyldiisopropylsilylethynyl)tetracene (NODIPS-Tc, Fig. 1a. By adding solvent to the liquid, we bridge between a material composed of neat chromophore, and solutions of separated, randomly-oriented chromophores. Careful analysis of the time-resolved photoluminescence of this material, both neat and in concentrated solution, reveals three spectral components. The third component, attributed to $^1(\mathrm{TT})$, becomes more prominent during TF, as expected from a simple kinetic model (details in Supplementary Materials). Furthermore, the spectrally-resolved magnetic field effect on the luminescence of this system reveals that luminescence enhancement is stronger at the wavelengths where the $^1(\mathrm{TT})$ emission is peaked. Enhanced photoluminescence in the $0-0$ band is interpreted in terms of TF by a pair state with chromophores oriented end-to-end, with weak excitonic coupling.[38] These experiments unite the observations of Dover *et al.* and Bossanyi *et al.*,[19,23] showing that there is a spectrally observable emissive intermediate in SF both in concentrated solutions and the solid state, but that this is distinct from the broad, red-shifted excimer emission.

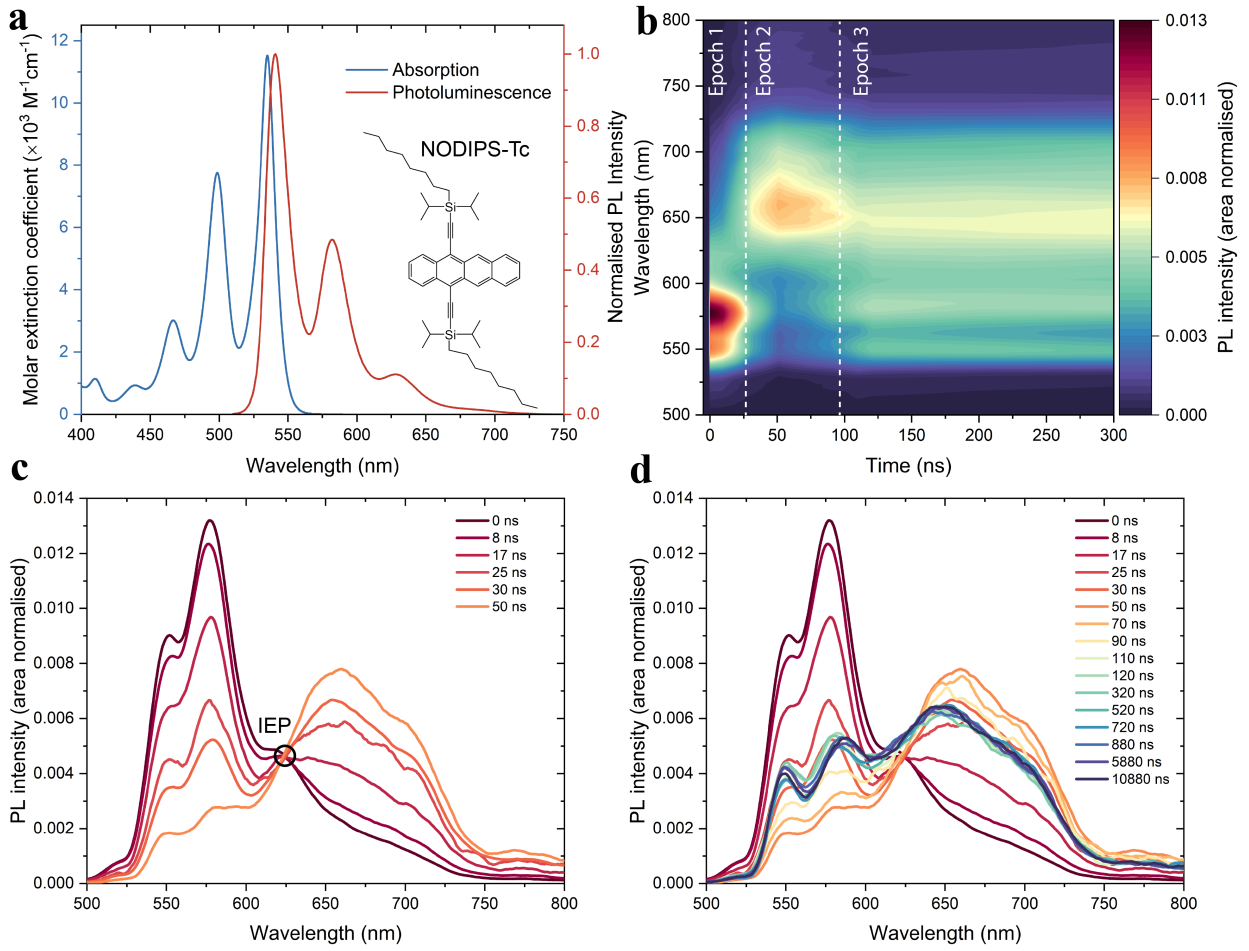

Figure 1: **Steady-state and time-resolved photoluminescence (TRPL) of NODIPS-Tc. a** Absorption and fluorescence spectrum of NODIPS-Tc in dilute solution and the chemical structure of NODIPS-Tc. **b** Normalized-spectrum heat map of TRPL after 532 nm laser excitation. **c** Area-normalized spectral slices illustrating the spectral dynamics at early times ($0 - 50$ ns). Note the clear iso-emissive point (IEP). **d** Spectral slices illustrating the spectral dynamics at all times ($0 - 10880$ ns).

Results

The room-temperature time-resolved photoluminescence (TRPL) of neat NODIPS-Tc liquid is shown in Fig. 1b. Each spectrum is normalized by its integral, accentuating the changes that occur as the spectrum evolves in time. At early times (0 - 30 ns, Epoch 1), the emission is dominated by the photo-generated S_1 state, rapidly red-shifting into an ^{1}Ex-dominated spectral shape in Epoch 2 (30 - 100 ns). The S_1 emission appears H-aggregated,[38] with the $0 - 0$ band suppressed to a

greater extent than in more dilute (yet optically thick) samples measured under identical conditions (Supplementary Fig. 1). The expected effect of self-absorption on the spectra is shown in Supplementary Fig. 2. The early-time spectral slices spanning Epochs 1 and 2 are plotted in Fig. 1c, clearly exhibiting an iso-emissive point (IEP) near 625 nm. The presence of an IEP in the area-normalized spectra suggests that there are two major components that dominate the spectra. For comparison, the steady-state absorption and photoluminescence spectra of dilute NODIPS-Tc solution are shown in Fig. 1a.

Like with TIPS-Tc, in NODIPS-Tc, both SF and TF pathways are thermally accessible.[19,39] After 100 ns, in Epoch 3, the annihilation of SF-generated triplets dominates the spectrum. The spectral shape stabilises and exhibits both S_1 and $^1\mathrm{Ex}$ features. The long-time spectral dynamics are shown in Fig. 1d. It is clear that the emission spectrum deviates from the IEP, strongly suggesting the presence of a third spectral component. To quantify the presence of a third component, we implemented principal component analysis (PCA).

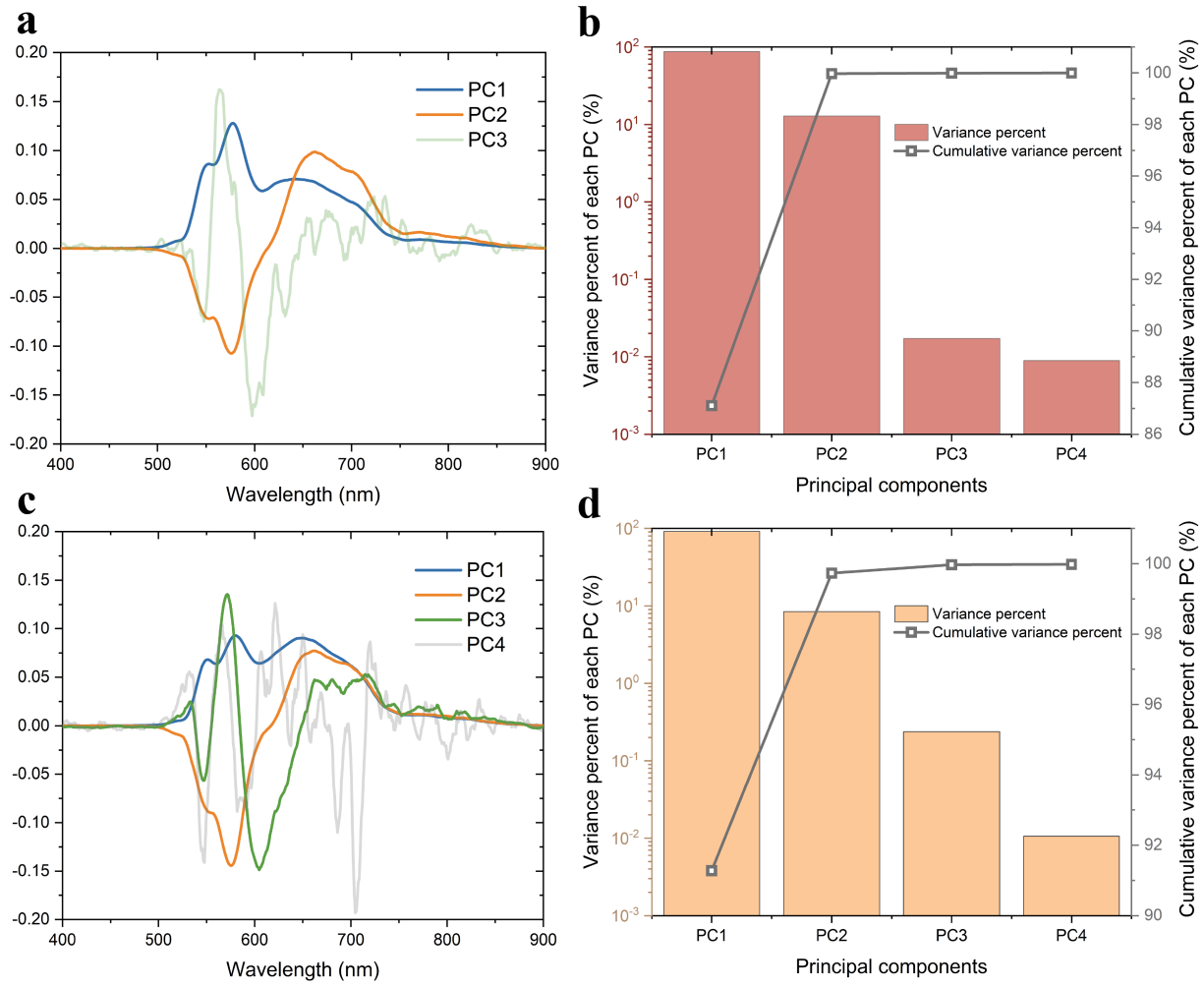

Figure 2: **Principal component analysis (PCA) on TRPL of neat NODIPS-Tc. a** Eigenvectors of the first three principal components of the early-time TRPL (0 - 50 ns). **b** Variance percent and cumulative variance percent of each principal component of early-time TRPL (0 - 50 ns). **c** Eigenvectors of the first four principal components of the long-time TRPL (0 - 10 μs). **d** Variance percent and cumulative variance percent of each principal component of long-time TRPL (0 - 10 μs).

The most important principal components (PCs) spanning Epochs 1 and 2 (Fig. 1c) are plotted in Fig. 2a. The percentage variance explained by each PC and the cumulative variance is plotted in Fig. 2b. At these early times, the first two PCs account for 99.97% of the total variance. It is important to note that PCA does not generate the spectra of species, and as the PCs are necessarily orthogonal, they can exhibit differently signed spectral regions. PC1 represents the average spectrum, and PC2 accounts for the changes, with the S_1 component diminishing and the

^{1}Ex component growing in time. The eigenvector of PC3 is noisy and its variance percent drops by a factor of 750 compared to PC2. As such, at this point we do not claim that PC3 represents a meaningful contribution to the spectra at early times.

The PCA of the entire data set is shown in Figs 2c and 2d. Clearly, PC3 is smoother and the variance ratio between the second and third PCs rises to about 35. Now the first three PCs contribute to 99.97% of the total variance and the fourth PC is very noisy. It only contributes 0.01% variance in both analyses.

The PCs can be used as a basis to reconstruct the experimental TRPL data, as shown in Supplementary Fig. 4 and Supplementary Fig. 5. At early times, the TRPL can be satisfactorily reconstructed by the first two PCs. However, reconstruction of the entire data set using only two PCs preserves the iso-emissive point, which is contrary to observations. Faithful reproduction of the salient experimental observation (the deviation from the iso-emissive point) necessitates the incorporation of the third PC (see Supplementary Fig. 5a and b). The residuals after reconstruction using only two PCs clearly show a distinct spectral feature, which is captured by the third PC. At this point it is instructive to note the similarity of the shape of the third component in both data sets, suggesting its smaller contribution at early times.

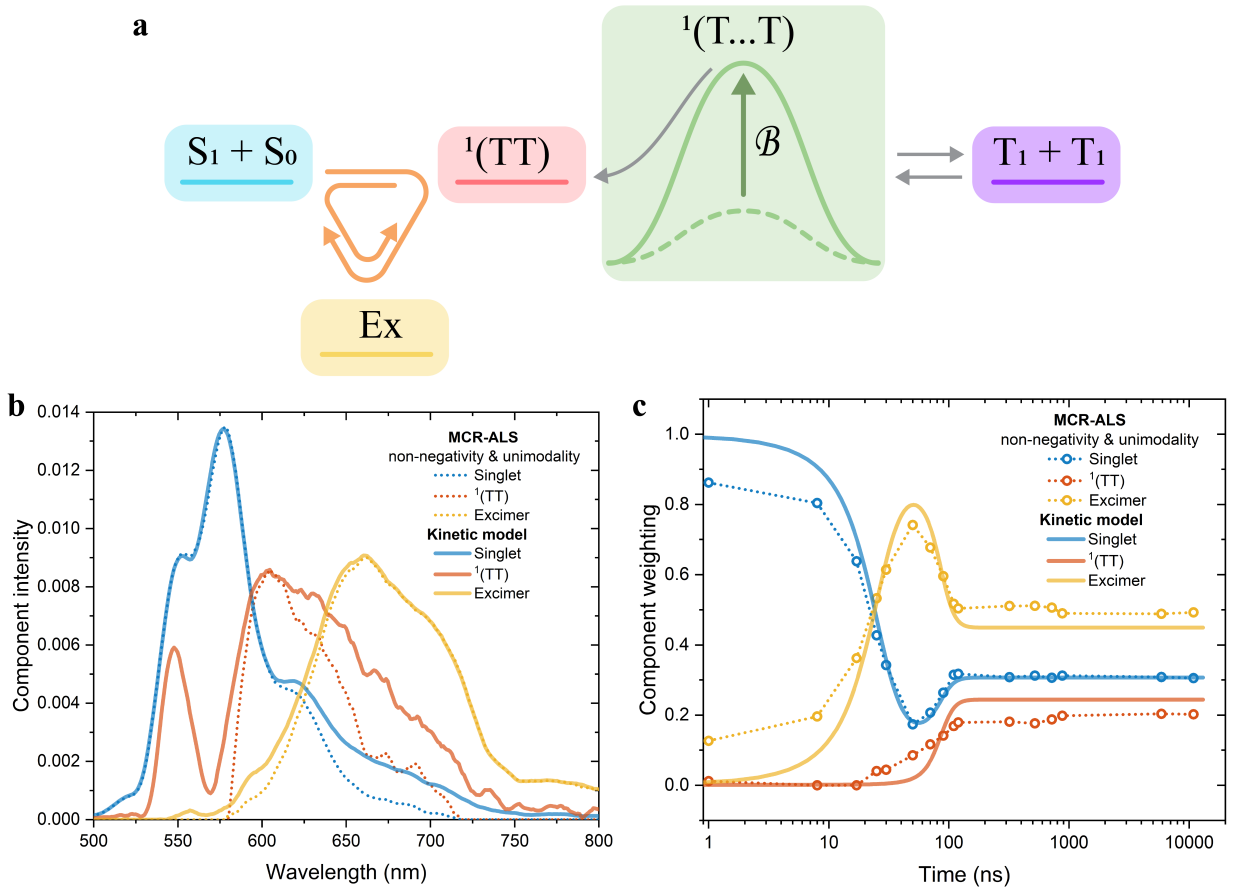

Figure 3: **Photoluminescence kinetics. a** The kinetic scheme shows the *quasi*-equilibrium formed between the S_1 state, ^{1}Ex and strongly exchange-coupled $^1(TT)$ state, and their connection to separated triplets. The external magnetic field, $\mathcal{B}$, modifies the Gibbs free energy of activation for SF, giving rise to the magnetic-field effect on photoluminescence. **b** Spectra fit to kinetic model, and extracted using the MCR-ALS algorithm.[40] **c** Kinetic model and MCR-ALS derived weightings of the spectra from **b** (details in the Supplementary Materials).

The number of PCs may be equated with the number of kinetically distinct emissive species. As such, three PCs implies at least three emissive species. Given that the S_1 and ^{1}Ex emission in Epoch 1 are largely explained by combinations of the first two PCs, we propose that the third component is due to emission by an excitonically coupled chromophore pair which is spectrally distinct from the Excimer. This state emits most prominently in Epoch 3, where it is fed directly by TF. As such, we assign this species to the exchange-coupled triplet pair state, $^1(TT)$, as reported in the solid state.[23,32,34,41,42] Emission from this state has never before been identified in a liquid system.

The relative prominence of the $^1(\mathrm{TT})$ state during the TF phase is supported by a minimal kinetic model, where the three emissive states, S_1, $^1\mathrm{Ex}$ and $^1(\mathrm{TT})$ are connected through $^1(\mathrm{TT})$ to a pool of free triplets, T_1, via the SF and TF processes. The model is illustrated by Fig. 3a but omits the intermediate $^1(\mathrm{T}\ldots\mathrm{T})$ state, which is absorbed into the rate constants for SF and TF. Details are given in the Supplementary Materials. The parameters describing the kinetic model and the spectra of the S_1, $^1\mathrm{Ex}$ and $^1(\mathrm{TT})$ states were globally fit to the data in Fig. 1d. The spectra are plotted in Fig. 3b, with the time-dependent weightings shown in Fig. 3c.

Using the MCR-ALS algorithm[40] under the constraints of non-negativity and unimodality, the dynamics are remarkably similar. However, the MCR-ALS extracted spectrum for the $^1(\mathrm{TT})$ state does not reproduce the sharp peak at 550 nm. Nevertheless, the salient features of the dynamics are that the S_1 state decays and generates the $^1\mathrm{Ex}$ state. The spectral contribution of the latter peaks, and as the system shifts into the TF phase (Epoch 3), the $^1(\mathrm{TT})$ state spectral contribution rises.

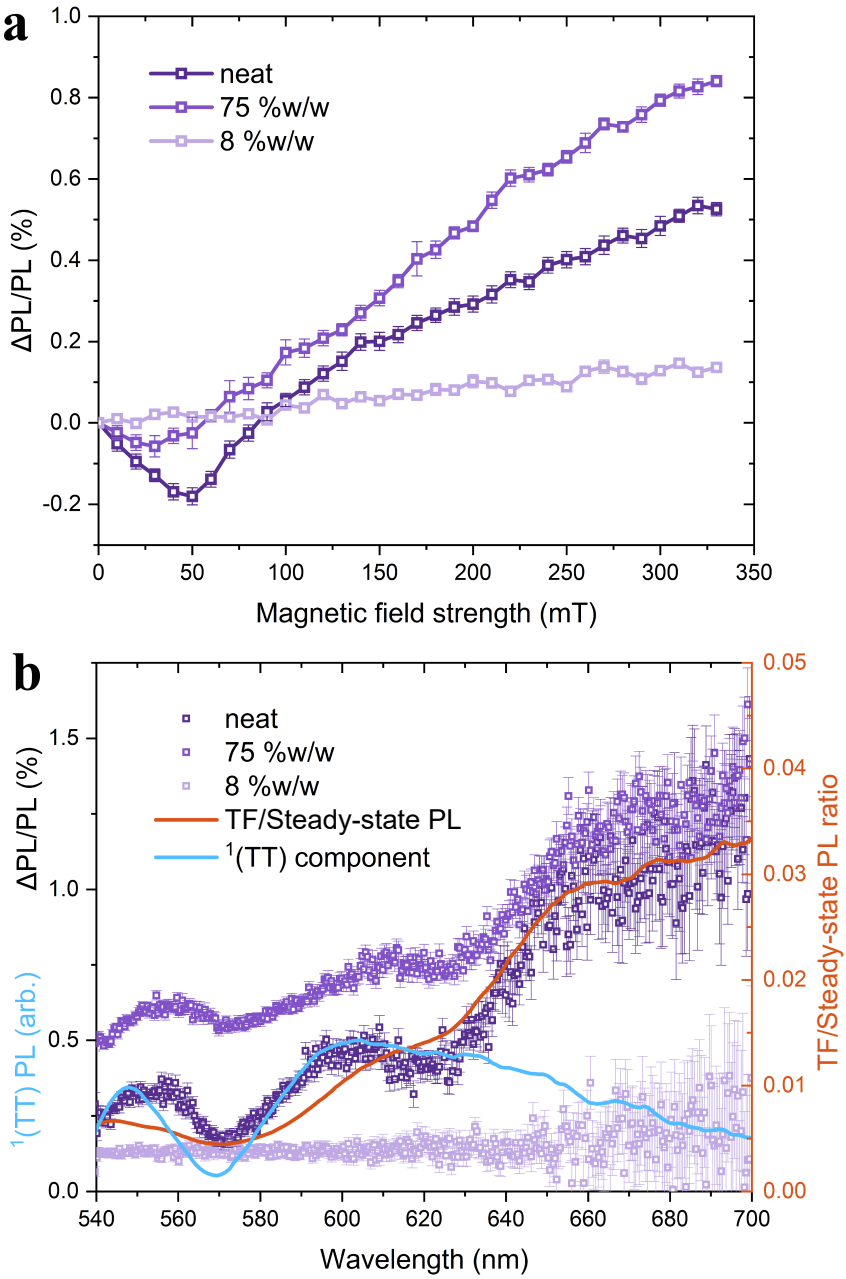

Figure 4: **The magnetic field effect (MFE) on photoluminescence of NODIPS-Tc.** **a** Effect of magnetic field (0 - 330 mT) on the integrated PL of NODIPS-Tc at three concentrations. **b** Wavelength-dependence of the magnetic-field effect on the PL of NODIPS-Tc at 330 mT magnetic field. The vertical axis is expressed in the percentage PL change (ΔPL/PL). For comparison, we plot the $^1(\mathrm{TT})$ spectrum from Fig. 3b (blue), and the ratio of the TF spectrum from Epoch 3 to the steady-state photoluminescence (orange).

To shed further light on the spectral characteristics of the $^1(\mathrm{TT})$ state, we performed magnetic field experiments. Though not directly observable through photoluminescence, there must also

be a bichromophoric state where the exchange coupling is weaker than the zero-field splitting, $^1(\mathrm{T}\ldots\mathrm{T})$. This weakly-coupled regime is included in the kinetic scheme illustrated in Fig. 3a. For aligned chromophores, at zero-field there are three out of nine triplet pair sub-levels with singlet character ($|xx\rangle$, $|yy\rangle$ and $|zz\rangle$, where the triplet basis is $\{|x\rangle, |y\rangle, |z\rangle\}$). As a magnetic field is applied, these states mix with other sub-levels and the number of levels with singlet character increases, essentially increasing the entropy of the $^1(\mathrm{T}\ldots\mathrm{T})$ state. At higher fields where the basis transforms into $\{|-\rangle, |0\rangle, |+\rangle\}$, only two of the nine weakly-coupled sub-states have singlet character, $|00\rangle$ and $(|+-\rangle + |-+\rangle)/\sqrt{2}$, and the entropy of the state is diminished.[36,43–45] Low entropy of an intermediate is accompanied by a higher free energy of activation, and thus rate constants are effectively manipulated by the magnetic field (see Supplementary Materials). This effect of the magnetic field on the free energy of the $^1(\mathrm{T}\ldots\mathrm{T})$ state is illustrated schematically in Fig. 3a.

The effect of increasing the free energy of the $^1(\mathrm{T}\ldots\mathrm{T})$ state is to attenuate SF, and thus enhance photoluminescence. In Fig. 4a, we see that at fields as high as 300 mT, for the neat sample, the photoluminescence is enhanced by about 0.5 % (ΔPL/PL). Furthermore, we see that at low fields, the photoluminescence is diminished, which is characteristic of chromophores that are aligned on the time-scales of SF and TF. This alignment is itself less evident but persists in the 75 % w/w sample. In the most dilute sample, both the alignment effect and the SF rate are diminished, giving rise to a smaller positive magnetic field effect at all fields.

We expect each spectrum identified in TRPL to have a different magnetic field dependence. Raising the free energy of the $^1(\mathrm{T}\ldots\mathrm{T})$ state with a magnetic field should enhance the emission non-uniformly by returning population initially to the $^1(\mathrm{TT})$ state. This is indeed found to be the case. The ΔPL/PL(λ) is shown in Fig. 4b. The neat and concentrated samples both exhibit peaks around 555 nm and 600 nm. It also clearly shows more enhancement at longer wavelengths which is attributable to excimer emission. Population returned to an uncoupled S_1 state by the action of the magnetic field can be expected to have an identical fate to photogenerated S_1 chromophores, and thus the enhanced emission will be identical to the steady-state emission. This is what is

seen at the most dilute concentration. In the most dilute solution, as opposed to the neat sample, molecular collisions resulting in SF or TF may occur at geometries that are not predisposed to excimer formation. However, in the neat sample, where the chromophores are aligned, there is clearly excess excimer emission generated by the magnetic field. This is evidence for a direct route from the $^1(\mathrm{TT})$ state to the $^1\mathrm{Ex}$ state, as included in the simple kinetic model.

TF feeds the photophysical network from the $^1(\mathrm{T}\ldots\mathrm{T})$ state, and as such, we would expect, as a first approximation, that the magnetic enhancement would be identical to the spectrum observed during Epoch 3, where TF dominates. The ratio of the TF spectrum in Epoch 3 to the steady-state spectrum is plotted in Fig. 4b. While an imperfect match, it exhibits the same shape, with excess $^1\mathrm{Ex}$ emission and a minimum at 570 nm. While the minimum at 620 nm is absent, there is a clear shoulder in its place. The differences suggest that the generation and recombination of geminate $^1(\mathrm{T}\ldots\mathrm{T})$ pairs does not produce the exact same spectrum as TF from uncorrelated triplets. Nevertheless, we may use the magnetic enhancement to gain insight into the spectrum generated by the emissive $^1(\mathrm{TT})$ state.

The $^1(\mathrm{TT})$-associated spectrum generated from the kinetic model (Fig. 3b) is also plotted in Fig. 4b. The peaks around 555 nm and 600 nm align with the magnetic $\Delta\mathrm{PL}$. The 600 nm feature does not align with either the S_1 or $^1\mathrm{Ex}$ states, and is thus attributed to the $^1(\mathrm{TT})$ state. The excess $^1\mathrm{Ex}$ can be attributed to fusion of a triplet pair that is predisposed to excimer formation. Since the magnetic field response indicates chromophore alignment, we attribute this to a stacked triplet pair. However, there are other conceivable triplet pairs from which fusion to S_1 would not generate more excimer than the steady-state spectrum. Of these pairs, a side-to-side arrangement of chromophores would appear frustrated by the bulky NODIPS groups. However, an end-to-end arrangement will exhibit weak excitonic coupling and, like the free chromophore, is expected to generate $0-0$ emission more prominently than the H-aggregated steady-state emission.[38] This accounts for the enhanced emission observed at 555 nm as compared to the steady-state emission. This is a feature of TF and is thus kinetically indistinct from the $^1(\mathrm{TT})$ emission. Both the spectrum derived from kinetic modelling and the MFE-derived spectrum contain features which can be ascribed to TF-

induced 0–0 emission and the $^1(\mathrm{TT})$ state respectively.

Conclusion

In this work, we analysed the time-resolved emission of NODIPS-tetracene, a liquid-state SF and TF material. As seen in other systems, the photogenerated bright state generates excimers which emit with an unstructured, red-shifted spectrum. In the first 50 ns, the normalized spectra exhibit an iso-emissive point, indicating the presence of two major spectral components. At longer times, during the TF phase, a third spectral component is identified. This is confirmed by principal component analysis.

Kinetic modelling and MCR-ALS analysis reveal that the third component is most prevalent during the TF phase. Further insight into the spectral components generated by a triplet-pair is gained from magnetic field experiments. Photoluminescence enhancement is observed at 555 nm and 600 nm, as well as in the excimer spectrum, as compared to the steady-state spectrum. This is attributed in part to TF from a stacked triplet pair which is then predisposed to excimer formation. The 600 nm emission, which is distinct from the S_1 and $^1\mathrm{Ex}$ spectra, is assigned to the $^1(\mathrm{TT})$ state itself. The 555 nm emission is interpreted in terms of triplet chromophores arranged such that they preferentially emit in the $0-0$ band compared to the steady-state spectrum, due to decreased excitonic coupling.

The results in this work underscore the complexity of the excited states in the most studied SF chromophore (tetracene). In addition to unifying the debate about the fundamental photophysics of SF and TF, our results have many implications for technologies which exploit SF and TF. First, multiexciton logic and magnetic resonance imaging are underpinned by an understanding of spin evolution and is affected by the equilibrium in Fig 3a. Second, the development of TF-based LEDs necessitate an understanding of all the emissive states in the system. Finally, magnetic field dependent measurements are often used to characterise SF-based solar cells.[5,46,47] These analyses usually assume that the magnetic field perturbs the equilibrium between just two electronic states

(S_0S_1 and $T + T$), however as shown in Fig. 4, this is an oversimplication.

These results highlight several features of SF and TF systems in general. They further show that the excimer state is not a necessary intermediate in SF or TF, but serves as a trap. Furthermore, it is shown that emission from the $^1(TT)$ state can be observed at room temperature in non-solid-state systems, and that this emission is enhanced by a magnetic field more so than the steady-state emission. In more dilute solutions of chromophore, these effects are less evidential.

Methods

Chemical Synthesis See Supplementary Materials for full details of the synthetic procedures.[48–50]

Sample preparation All samples used for TRPL spectroscopy were measured under an inert atmosphere using a Teflon-stopcock sealed quartz cuvette with a 1 mm path length. Toluene was added for diluted samples.

Optical spectroscopy Time-resolved photoluminescence spectroscopy (TRPL) was carried out using a SpitLight Picolo, ND:YVO^4 laser system with pulse duration of 800 ps at a repetition rate of 1 kHz and wavelength of 532 nm. Photoluminescence was detected using a spectrometer (Princeton Instruments 2300i) equipped with a 300 groove-per-millimetre grating blazed at 500 nm, and an intensified time-gated camera (Princeton Instruments Pi Max-4).

Steady-state optical absorption spectroscopy was performed with a Cary 60 UV-Visible-NIR spectrometer covering a wavelength range of 190-1100 nm.

For steady-state photoluminescence measurements, samples were excited by a 532 nm continuous-wave (CW) laser. The photoluminescence was collected an imaged onto a multi-mode optical fibre by two off-axis parabolic mirrors. An Ocean Optics Flame spectrometer was used to collect the photoluminescence spectrum.

Principal component analysis (PCA) Principal component analysis (PCA) was used to extract the emissive species (principal components) contributing to the time-resolved photoluminescence (TRPL). These principal components form a new basis set and can be used to reconstruct the exper-

imental data. An introduction to PCA can be found in this paper[51] (Shlens, Jonathon. "A tutorial on principal component analysis." arXiv preprint arXiv:1404.1100 (2014).) All PCA calculations were performed using custom-made Python code. Here we briefly outline the procedures for how PCA was performed.

Firstly, the experimental TRPL data set was organised as an $m \times n$ matrix X, where m is the number of measurement types, i.e. dimensions (in this case the number of wavelengths) and n is the number of observations (in this case the number of time series). Secondly, the covariance matrix $C = XX^T$ was computed, where C is a square symmetric $m \times m$ matrix. The diagonal terms of C are the variance of each measurement type and the off-diagonal terms are the covariance between measurement types. C matrix contains the correlations between all possible pairs of measurements. Thirdly, eigendecomposition of the covariance matrix C was performed, which yields the eigenvectors of principal components (PCs) and eigenvalues, i.e. the variance of each PC. These PCs constitute a new basis set of the original data.

We can thus reconstruct the experimental data using this new basis set. We firstly construct a matrix V from the eigenvectors of k number of PCs, where V is the $m \times k$ matrix. Then we define the projection matrix VV^T and the reconstructed data is given by $X_{reconstructed} = (X^T VV^T)^T$. The residual data is given by $X_{residual} = X - X_{reconstructed}$ for each observation. We can also compute the reconstruction loss using the mean squared error between the experimental data and the reconstructed data: reconstruction loss = $1/N \sum_{n=1}^{N} \|x_n - \tilde{x}_n\|^2$, where x_n is the experimental data and $\tilde{x}_n$ is the reconstructed data.

Data Availability

The data that support the findings of this study are available from the corresponding author upon reasonable request.

Acknowledgements

This work was supported by the Australian Research Council (Centre of Excellence in Exciton Science CE170100026).

Author Contributions

JF, PH, SKKP and DdC performed the measurements. TWS, JF, PH, MJYT, JHC, NJE-D and MPN analysed the results. MWB, AF, SNS, JEB, HLL and PT synthesized and analysed the NODIPS-Tc material. TWS and JF wrote the manuscript. JF designed the figures. TWS designed the study, and performed the kinetic modelling.

Competing Financial Interests

There are no competing financial interests.

References

(1) Smith, M. B.; Michl, J. Recent Advances in Singlet Fission. *Annu. Rev. Phys. Chem.* **2013**, *64*, 361–386.

(2) Feng, J.; Alves, J.; de Clercq, D. M.; Schmidt, T. W. Photochemical Upconversion. *Annu. Rev. Phys. Chem.* **2023**, *74*, 145–168.

(3) Schulze, T. F.; Schmidt, T. W. Photochemical upconversion: present status and prospects for its application to solar energy conversion. *Energy Environ. Sci.* **2015**, *8*, 103–125.

(4) MacQueen, R. W.; Liebhaber, M.; Niederhausen, J.; Mews, M.; Gersmann, C.; Jäckle, S.; Jäger, K.; Tayebjee, M. J. Y.; Schmidt, T. W.; Rech, B.; Lips, K. Crystalline silicon solar cells

with tetracene interlayers: the path to silicon-singlet fission heterojunction devices. *Mater. Horiz.* **2018**, *5*, 1065–1075.

(5) Einzinger, M.; Wu, T.; Kompalla, J. F.; Smith, H. L.; Perkinson, C. F.; Nienhaus, L.; Wieghold, S.; Congreve, D. N.; Kahn, A.; Bawendi, M. G.; Baldo, M. A. Sensitization of silicon by singlet exciton fission in tetracene. *Nature* **2019**, *571*, 90–94.

(6) Ravetz, B. D.; Pun, A. B.; Churchill, E. M.; Congreve, D. N.; Rovis, T.; Campos, L. M. Photoredox catalysis using infrared light via triplet fusion upconversion. *Nature* **2019**, *565*, 343–346.

(7) Zhu, X.; Su, Q.; Feng, W.; Li, F. Anti-Stokes shift luminescent materials for bio-applications. *Chem. Soc. Rev.* **2017**, *46*, 1025–1039.

(8) Kawashima, Y. et al. Singlet fission as a polarized spin generator for dynamic nuclear polarization. *Nat. Commun. volume 14, Article number: 1056 (2023) Cite this article* **2023**, *14*, 1056.

(9) Jacobberger, R. M.; Qiu, Y.; Williams, M. L.; Krzyaniak, M. D.; Wasielewski, M. R. Using Molecular Design to Enhance the Coherence Time of Quintet Multiexcitons Generated by Singlet Fission in Single Crystals. *J. Am. Chem. Soc.* **2022**, *144*, 2276–2283.

(10) Hudson, R. J.; MacDonald, T. S. C.; Cole, J. H.; Schmidt, T. W.; Smith, T. A.; McCamey, D. R. A Framework for Multiexcitonic Logic. *Nat. Rev. Chem.* **2023**, in press.

(11) Sanders, S. N.; Schloemer, T. H.; Gangishetty, M. K.; Anderson, D.; Seitz, M.; Gallegos, A. O.; Stokes, R. C.; Congreve, D. N. Triplet fusion upconversion nanocapsules for volumetric 3D printing. *Nature* **2022**, *604*, 474–478.

(12) Tayebjee, M. J. Y.; McCamey, D. R.; Schmidt, T. W. Beyond Shockley–Queisser: Molecular Approaches to High-Efficiency Photovoltaics. *J. Phys. Chem. Lett.* **2015**, *6*, 2367–2378.

(13) Tayebjee, M. J. Y.; Gray-Weale, A. A.; Schmidt, T. W. Thermodynamic Limit of Exciton Fission Solar Cell Efficiency. *J. Phys. Chem. Lett.* **2012**, *3*, 2749–2754.

(14) Rao, A.; Friend, R. H. Harnessing singlet exciton fission to break the Shockley–Queisser limit. *Nature reviews materials* **2017**, *2*, 1–12.

(15) Pensack, R. D.; Ostroumov, E. E.; Tilley, A. J.; Mazza, S.; Grieco, C.; Thorley, K. J.; Asbury, J. B.; Seferos, D. S.; Anthony, J. E.; Scholes, G. D. Observation of Two Triplet-Pair Intermediates in Singlet Exciton Fission. *J. Phys. Chem. Lett.* **2016**, *7*, 2370–2375.

(16) Bakulin, A. A.; Morgan, S. E.; Kehoe, T. B.; Wilson, M. W.; Chin, A. W.; Zigmantas, D.; Egorova, D.; Rao, A. Real-time observation of multiexcitonic states in ultrafast singlet fission using coherent 2D electronic spectroscopy. *Nat. Chem.* **2016**, *8*, 16–23.

(17) Monahan, N. R.; Sun, D.; Tamura, H.; Williams, K. W.; Xu, B.; Zhong, Y.; Kumar, B.; Nuckolls, C.; Harutyunyan, A. R.; Chen, G., et al. Dynamics of the triplet-pair state reveals the likely coexistence of coherent and incoherent singlet fission in crystalline hexacene. *Nat. Chem.* **2017**, *9*, 341–346.

(18) Burdett, J. J.; Bardeen, C. J. Quantum beats in crystalline tetracene delayed fluorescence due to triplet pair coherences produced by direct singlet fission. *J. Am. Chem. Soc.* **2012**, *134*, 8597–8607.

(19) Dover, C. B.; Gallaher, J. K.; Frazer, L.; Tapping, P. C.; Petty, A. J.; Crossley, M. J.; Anthony, J. E.; Kee, T. W.; Schmidt, T. W. Endothermic singlet fission is hindered by excimer formation. *Nature chemistry* **2018**, *10*, 305–310.

(20) Walker, B. J.; Musser, A. J.; Beljonne, D.; Friend, R. H. Singlet exciton fission in solution. *Nature chemistry* **2013**, *5*, 1019–1024.

(21) Stern, H. L.; Musser, A. J.; Gelinas, S.; Parkinson, P.; Herz, L. M.; Bruzek, M. J.; Anthony, J.;

Friend, R. H.; Walker, B. J. Identification of a triplet pair intermediate in singlet exciton fission in solution. *Proceedings of the National Academy of Sciences* **2015**, *112*, 7656–7661.

(22) Dvořák, M.; Prasad, S. K. K.; Dover, C. B.; Forest, C. R.; Kaleem, A.; MacQueen, R. W.; Petty, A. J. I.; Forecast, R.; Beves, J. E.; Anthony, J. E.; Tayebjee, M. J. Y.; Widmer-Cooper, A.; Thordarson, P.; Schmidt, T. W. Singlet Fission in Concentrated TIPS-Pentacene Solutions: The Role of Excimers and Aggregates. *J. Am. Chem. Soc.* **2021**, *143*, 13749–13758.

(23) Bossanyi, D. G.; Matthiesen, M.; Wang, S.; Smith, J. A.; Kilbride, R. C.; Shipp, J. D.; Chekulaev, D.; Holland, E.; Anthony, J. E.; Zaumseil, J., et al. Emissive spin-0 triplet-pairs are a direct product of triplet–triplet annihilation in pentacene single crystals and anthradithiophene films. *Nature chemistry* **2021**, *13*, 163–171.

(24) Ryerson, J. L.; Schrauben, J. N.; Ferguson, A. J.; Sahoo, S. C.; Naumov, P.; Havlas, Z.; Michl, J.; Nozik, A. J.; Johnson, J. C. Two Thin Film Polymorphs of the Singlet Fission Compound 1,3-Diphenylisobenzofuran. *J. Phys. Chem. C* **2014**, *118*, 12121–12132.

(25) Schrauben, J. N.; Ryerson, J. L.; Michl, J.; Johnson, J. C. Mechanism of Singlet Fission in Thin Films of 1,3-Diphenylisobenzofuran. *J. Amer. Chem. Soc.* **2014**, *136*, 7363–7373.

(26) Feng, X.; Krylov, A. I. On couplings and excimers: lessons from studies of singlet fission in covalently linked tetracene dimers. *Phys. Chem. Chem. Phys.* **2016**, *18*, 7751–7761.

(27) Mauck, C. M.; Hartnett, P. E.; Margulies, E. A.; Ma, L.; Miller, C. E.; Schatz, G. C.; Marks, T. J.; Wasielewski, M. R. Singlet fission via an excimer-like intermediate in 3, 6-bis (thiophen-2-yl) diketopyrrolopyrrole derivatives. *J. Am. Chem. Soc.* **2016**, *138*, 11749–11761.

(28) Burdett, J. J.; Gosztola, D.; Bardeen, C. J. The dependence of singlet exciton relaxation on excitation density and temperature in polycrystalline tetracene thin films: Kinetic evidence for a dark intermediate state and implications for singlet fission. *The Journal of chemical physics* **2011**, *135*, 214508.

(29) Tayebjee, M. J.; Clady, R. G.; Schmidt, T. W. The exciton dynamics in tetracene thin films. *Physical Chemistry Chemical Physics* **2013**, *15*, 14797–14805.

(30) Grieco, C.; Kennehan, E. R.; Kim, H.; Pensack, R. D.; Brigeman, A. N.; Rimshaw, A.; Payne, M. M.; Anthony, J. E.; Giebink, N. C.; Scholes, G. D.; Asbury, J. B. Direct Observation of Correlated Triplet Pair Dynamics during Singlet Fission Using Ultrafast Mid-IR Spectroscopy. *J. Phys. Chem. C* **2018**, *122*, 2012–2022.

(31) Understanding the Bound Triplet-Pair State in Singlet Fission. *Chem* **2019**, *5*, 1988–2005.

(32) Hausch, J.; Berges, A. J.; Zeiser, C.; Rammler, T.; Morlok, A.; Bredehöft, J.; Hammer, S.; Pflaum, J.; Bardeen, C. J.; Broch, K. Distinguishing between Triplet-Pair State and Excimer Emission in Singlet Fission Chromophores Using Mixed Thin Films. *J. Phys. Chem. C* **2022**, *126*, 6686–6693.

(33) Miyata, K.; Conrad-Burton, F. S.; Geyer, F. L.; Zhu, X.-Y. Triplet Pair States in Singlet Fission. *Chem. Rev.* **2019**, *119*, 4261–4292.

(34) Yong, C. K.; Musser, A. J.; Bayliss, S. L.; Lukman, S.; Tamura, H.; Bubnova, O.; Hallani, R. K.; Meneau, A.; Resel, R.; Maruyama, M., et al. The entangled triplet pair state in acene and heteroacene materials. *Nature communications* **2017**, *8*, 15953.

(35) Lukman, S.; Richter, J. M.; Yang, L.; Hu, P.; Wu, J.; Greenham, N. C.; Musser, A. J. Efficient Singlet Fission and Triplet-Pair Emission in a Family of Zethrene Diradicaloids. *J. Am. Chem. Soc.* **2017**, *139*, 18376–18385.

(36) Merrifield, R.; Avakian, P.; Groff, R. Fission of singlet excitons into pairs of triplet excitons in tetracene crystals. *Chem. Phys. Lett.* **1969**, *3*, 155–157.

(37) Wakasa, M.; Kaise, M.; Yago, T.; Katoh, R.; Wakikawa, Y.; Ikoma, T. What can be learned from magnetic field effects on singlet fission: Role of exchange interaction in excited triplet pairs. *The Journal of Physical Chemistry C* **2015**, *119*, 25840–25844.

(38) Hestand, N. J.; Spano, F. C. Expanded Theory of H- and J-Molecular Aggregates: The Effects of Vibronic Coupling and Intermolecular Charge Transfer. *Chemical Reviews* **2018**, *118*, 7069–7163.

(39) Bayliss, S. L.; Chepelianskii, A. D.; Sepe, A.; Walker, B. J.; Ehrler, B.; Bruzek, M. J.; Anthony, J. E.; Greenham, N. C. Geminate and nongeminate recombination of triplet excitons formed by singlet fission. *Physical review letters* **2014**, *112*, 238701.

(40) Jaumot, J.; Gargallo, R.; De Juan, A.; Tauler, R. A graphical user-friendly interface for MCR-ALS: a new tool for multivariate curve resolution in MATLAB. *Chemometrics and intelligent laboratory systems* **2005**, *76*, 101–110.

(41) Musser, A. J.; Clark, J. Triplet-pair states in organic semiconductors. *Annual review of physical chemistry* **2019**, *70*, 323–351.

(42) Stern, H. L.; Cheminal, A.; Yost, S. R.; Broch, K.; Bayliss, S. L.; Chen, K.; Tabachnyk, M.; Thorley, K.; Greenham, N.; Hodgkiss, J. M., et al. Vibronically coherent ultrafast triplet-pair formation and subsequent thermally activated dissociation control efficient endothermic singlet fission. *Nature chemistry* **2017**, *9*, 1205–1212.

(43) Johnson, R. C.; Merrifield, R. E. Effects of Magnetic Fields on the Mutual Annihilation of Triplet Excitons in Anthracene Crystals. *Phys. Rev. B* **1970**, *1*, 896–902.

(44) Johnson, R. C.; Merrifield, R. E.; Avakian, P.; Flippen, R. B. Effects of Magnetic Fields on the Mutual Annihilation of Triplet Excitons in Molecular Crystals. *Phys. Rev. Lett.* **1967**, *19*, 285–287.

(45) Merrifield, R. E. Theory of Magnetic Field Effects on the Mutual Annihilation of Triplet Excitons. *J. Chem. Phys.* **1968**, *48*, 4318–4319.

(46) Daiber, B.; Maiti, S.; Ferro, S. M.; Bodin, J.; van den Boom, A. F. J.; Luxembourg, S. L.; Kinge, S.; Pujari, S. P.; Zuilhof, H.; Siebbeles, L. D. A.; Ehrler, B. Change in Tetracene

Polymorphism Facilitates Triplet Transfer in Singlet Fission-Sensitized Silicon Solar Cells. *J. Phys. Chem. Lett.* **2020**, *11*, 8703–8709.

(47) Congreve, D. N.; Lee, J.; Thompson, N. J.; Hontz, E.; Yost, S. R.; Reusswig, P. D.; Bahlke, M. E.; Reineke, S.; Voorhis, T. V.; Baldo, M. A. External Quantum Efficiency Above 100% in a Singlet-Exciton-Fission–Based Organic Photovoltaic Cell. *Science* **2013**, *340*, 334–337.

(48) Kumarasamy, E.; Sanders, S. N.; Pun, A. B.; Vaselabadi, S. A.; Low, J. Z.; Sfeir, M. Y.; Steigerwald, M. L.; Stein, G. E.; Campos, L. M. Properties of Poly- and Oligopentacenes Synthesized from Modular Building Blocks. *Macromol.* **2016**, *49*, 1279–1285.

(49) Jennings, W. B. Chemical shift nonequivalence in prochiral groups. *Chem. Rev.* **1975**, *75*, 307–322.

(50) McFarlane, W. Chemical shift and coupling constant nonequivalence of isopropyl methyl protons in a tertiary phosphine. *Chem. Commun.* **1968**, 229–230.

(51) Shlens, J. A tutorial on principal component analysis. *arXiv preprint arXiv:1404.1100* **2014**,

Supplementary Materials

Supplementary Text

Supplementary Figures 1 to 9

Supplementary Table

Supplementary Scheme